Imaging shallow objects with scattered guided waves

Gérard C. Herman, Delft University, Paul A. Milligan, UC Berkeley, Robert Huggins, Geometrics Inc., James W. Rector III,* UC *Berkeley*

SUMMARY

Current surface seismic reflection techniques based on the common-mid-point (CMP) reflection stacking method can not be readily used to image small objects in the first few meters of the weathered layer. We discuss a seismic imaging method which uses the fist-arrjval (guided) wave, scattered by shallow heterogeneities and converted into scattered Rayleigh waves, to detect such objects. These guided waves and Rayleigh waves are dominant in the shallow weathered layer, and are thus suitable for shallow object imaging. We applied this method to a field data set and found that we could certainly image meter-size objects up to about 3 m off to the side of a survey line consisting of vertical geophones. There are indications that crossline horizontal geophone data could be used to identify shallow objects up to 10 m off line in the same region.

INTRODUCTION

Use of the surface seismic reflection method (Steeples et al., 1997), based on common-mid-point (CMP) reflection gathers and stacking to image the very shallow subsurface, is often limited by the early record times being dominated by different types of strong and coherent guided wave modes trapped in the weathered layer. Examples of these guided waves are the Rayleigh waves, and the first arrivals refracted at a shallow interface and reflected multiple times by the free surface.

In this paper, we present a method for the imaging of acoustic impedance heterogeneities in the shallow weathered layer by using these strong guided wave modes. We conducted a field experiment involving burial of an empty drum to act as a secondary source of scattered Rayleigh waves and using the first arrival as the illuminating wave. We have processed these data to see if we could detect the presence of the drum.

In an earlier paper (Blonk et al., 1995), it was already found that Rayleigh waves can be employed for imaging a large object (a dam) at a distance of 150 m in a tidal flat region, whereas it appeared possible to image scatterers in a carstified near-surface region at distances of more than 1 km. In the present paper, we concentrate on the imaging of small (meter-size) objects at relatively close distances from the receivers (typically less than 10 m) in a region where a significant amount of very shallow near-surface scattering takes place. This somewhat different objective has consequences for the data processing method that are outlined in the present paper.

DESCRIPTION OF THE METHOD

We consider scattering of guided waves by shallow subsurface inhomogeneities that are relatively small with respect to the wavelength. The wavefield is generated by a source at surface position $\mathbf{x}^s$ and is recorded by vertical geophones at surface position x. Starting from the frequency-domain form of the elastodynamic wave equation, one can derive a domain-type integral representation for the vertical component of the particle velocity, v. It is given by

$$v(\omega, \mathbf{x}, \mathbf{x}^s) = v^0(\omega, \mathbf{x}, \mathbf{x}^s) + v^1(\omega, \mathbf{x}, \mathbf{x}^s), \qquad (1)$$

where w denotes the angular frequency, the incident field v^0 is the wavefield that would be present in the absence of scattering objects and the scattered field v^1 accounts for the presence of these objects. In our case, the offset between shot location and nearest receiver is chosen large enough, so that the first arrival is separated in time from the air wave and Rayleigh-wave modes. This fist arrival can be a refracted wave, that, after multiple bounces at the free surface, has become a guided wave, propagating mainly in the layer above the refracting interface. We consider the first arrival as the incident field. For shallow objects, the scattered field can be expressed in terms of the scattering impedance ξ by the relation

$$v^1(\mathbf{x}, \mathbf{x}^s) = \int_{\text{surface}} dA(\mathbf{x}')\, \xi(\mathbf{x}')\, V^G(\mathbf{x} - \mathbf{x}')\, v(\mathbf{x}', \mathbf{x}^s), \qquad (2)$$

where the Green's function V^G is the vertical velocity due to an impulsive vertical pointforce. In Eq.(2), the ω dependence is omitted and it is assumed that the near surface, apart from the scattering objects (the "background"), is laterally invariant. The validity of this model has been discussed by Blonk et al. (1995). In principle, shallow scattering objects can now be determined by carrying out the following steps:

1. Separation of the incident (direct) wave v^0, in our case the first arrival, and the scattered wave v^1 by the same type of wavefield separation techniques also used in the processing of VSP and cross-well reflection data.
2. Determination of the Green's function V^G by either measuring or modeling.

3. Imaging of the impedance function ξ after removing the wave propagation effect from the source to an imaging point x and from this imaging point to the receivers.

DESCRIPTION OF THE EXPERIMENT

The experiment was carried out at the Richmond Field Station of the University of California at Berkeley. The objective was, to investigate to what extent meter-size objects could be detected in the shallow subsurface using the technique of guided-wave imaging. The terrain, situated in the Bay margin, can be characterized as a muddy wetland, overgrown with grass and a few small bushes. The upper 30 m of the subsurface consist of tertiary muds; the water table is at l-2 m depth. The data-acquisition geometry is shown in figure 1. Both vertical and cross-line horizontal geophones were used. A vertical impact, inline, Betsy gun (8 gauge shells) was used as a source. The experiment using the vertical phones was carried out twice. First, shot records were recorded for six different shot positions spaced 10 m apart; the closest shot was situated 40 m from the first receiver. Then, an empty plastic drum having a diameter of about 0.6 m and a length of about 1 m was buried at a distance of 10 m and a depth of 1 m (oriented parallel to the line), after which the experiment was repeated with the same shot locations as before. The objective of this experiment was to compare the strength of the scattered field due to the drum with other near-surface scattering effects. For example, a bush having a diameter of about 1 m was present at a distance of about 3 m from the line. The position of the bush is also shown in figure 1. It was our intention to also perform the same pair of before and after experiments for the cross-line horizontal components, but, due to unforeseen circumstances, we were only able to record the cross-line horizontal data after the drum burial.

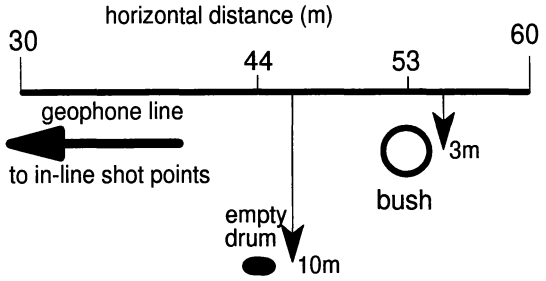

Figure 1: Planview of the experiment.

VERTICAL COMPONENT DATA

The processing sequences of the two vertical component data sets (before vs. after drum burial) were identical and along the lines indicated previously. A shot record, representative of the vertical component data both before and after burial of the drum is shown in figure 2. From the shot records, the scattered field v^1 has been estimated by applying a constrained eigenvector wavefield separation technique (Mars and Rector, 1995). In order to obtain an image of the scattering impedance function ξ, wave propagation effects from the sources and receivers to all surface locations have to be compensated for, followed by an imaging step (Blonk et al, 1995). For the imaging problem considered here, we are only interested in imaging objects closer than, say, 10 m from the line (which amounts to about 1 wavelength of the dominant frequency of the Rayleigh wave) and a less compute-intensive approach is possible if the velocities do not change too much over this short distance. As a first step, propagation time of the guided wave from the source to all points to be imaged is removed by subtracting the first-arrival times. Then, the scattered wavefields of several shotrecords are stacked (see figure 3). The back propagation of scattered Rayleigh waves between imaging points and receivers (related to the Green's function V^G of Eq.(2)

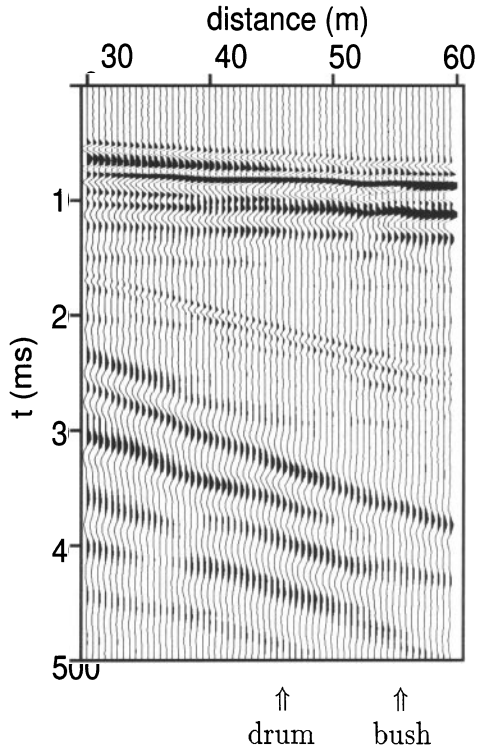

Figure 2: Typical shotrecord (vertical component data).

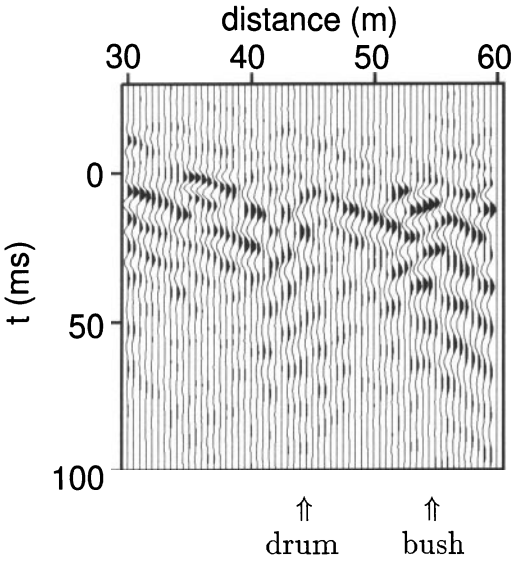

Figure 3: Scattered Rayleigh waves after removing incident wave, propagation time from the source and stacking shots (traces are aligned in time on the first-break picks).

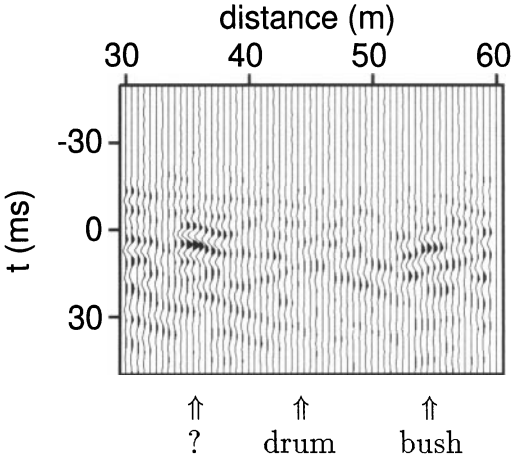

Figure 4: Near-surface impedance after imaging.

can also be simplified. To this aim, we assume all scattering objects to be lumped at the receiver line and discard the integration over the transverse horizontal direction (the y-direction). Furthermore, we have approximated the Green's function V^G by its one-dimensional form. In order to account for a proper amplitude decay, we have introduced attenuation. After imaging, all objects directly below the line will be imaged at time $t = 0$, whereas objects close to the line (at distances not exceeding a wavelength) will be imaged at somewhat later times τ, given by $\tau = \frac{y}{|c_R|}$, where y is the lateral distance of the object from the receiver line. In this way, objects directly below the receivers will still be imaged at $t = 0$, whereas objects at a few meters distance from the line will be imaged at later times. After imaging the scattered field by spatially deconvolving for the Green's function V^G and performing a temporal deconvolution for the total field v (see also Eq.(2), we obtain the impedance function shown in figure 4. At about 53 m, we see the image of the root-system of the bush at a traveltime of 8 ms, implying a horizontal distance of 2 m, which is consistent with the surface location of the bush. The width of the image is approximately l-2 m. There also appears to be another image at a horizontal receiver distance of 35 m. From the image time, we conclude that the crossline distance between the scattering object and the line is about 1.5 m. Since the object has no surface manifestation, we don't know what it is. The size seems to be l-2 m along the receiver line. There appears to be no image of the buried drum.

HORIZONTAL COMPONENT DATA

Due to the elliptic polarization of Rayleigh waves, crossline horizontal component geophones should be about as sensitive to crossline scattered Rayleigh waves as the vertical component geophones. But, at the same time, the crossline component is less sensitive to inline polarized waves, like the illuminating guided wave directly from the source (Blonk and Herman, 1996). The crossline component is also less sensitive to inline, or almost inline, scattered Rayleigh waves originating from heterogeneities close to the line (like the bush at 53 m in our case). Therefore, it should be possible to image objects somewhat further away using the crossline component. One of the crossline horizontal shotrecords after the drum burial is shown in figure 5. In principle, a similar processing sequence would be possible for the horizontal component data as for the vertical component data. But in our experiment, the horizontal component data quality was considerably inferior to the vertical component data, and good first-arrival picks could not be obtained. Therefore, the only processing carried out on the horizontal component data was the killing of bad traces followed by bandpass filtering and $f - x$ deconvolution to enhance spatial coherency and suppress noise.

The crossline-horizontal data shown in figure 5 has evidence of a diffraction tail, originating from the bush at 53 m, and of a faint hyperbola, centered at 44 m, with its apex arriving at about 120 ms (i.e., 40 ms after the first arrival). Using the Rayleigh-wave velocity of 240 m/s, this suggests a lateral distance of about 10 m. This hyperbola was also quite consistently visible on the other horizontal records. Unfortunately, we have not been

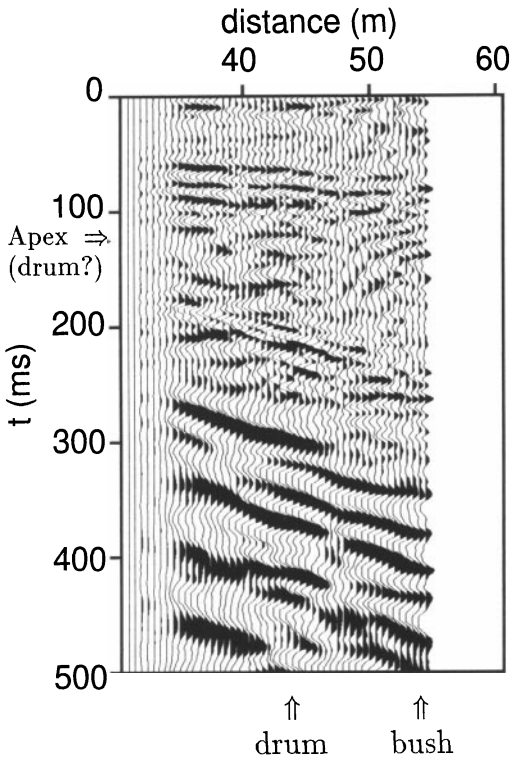

Figure 5: Crossline horizontal component data showing a faint diffraction hyperbola at the location of the drum. The apex is at 120 ms.

able to record the horizontal data prior to burial of the drum which implies no definite conclusions can be drawn whether or not this scattering hyperbola is due to the drum or to another heterogeneity. Nevertheless, it seems one can see objects up to a distance of 10m and that the crossline data is indeed more sensitive to crossline scattered Rayleigh waves than the vertical component data is.

CONCLUSIONS

We have discussed a method for imaging very shallow objects at relatively small distance from the receivers. As an illuminating wave, the first arrival (guided) wave is used. This illuminating wave is converted into scattered Rayleigh waves at shallow heterogeneities. From our experimental data, we found that we could use the vertical component data to image objects of size l-2 m at a maximum distance of 3 meters from the receiver line. Objects further away could not be imaged due to the dominant presence of scattered waves from these nearby heterogeneities.

The crossline horizontal data appears to be more sensitive to crossline scattered Rayleigh waves and less sensitive to the illuminating guided wave and in-line scattered waves. This type of data could therefore enable one to maybe detect objects somewhat further away, but the evidence is lacking to make firm statements based on this experiment. It is, however, consistent with earlier findings (Blonk and Herman, 1996). From other experiments, it was already found that the Rayleigh wave could also be used as the illuminating field (Blonk et al, 1995) and that a dam could be imaged at a distance of 150 m, whereas for another dataset, objects could be imaged at distances of more than 1 km. The possibility of detecting shallow objects is therefore very dependent upon the size of the object, their contrast, and the properties of the shallow subsurface, but there are definitely interesting possibilities to be investigated.

ACKNOWLEDGMENTS

This research has been carried out while Gerard Herman was a Phoebe Apperson Hearst visiting professor in the Department of Materials Science and Mineral Engineering with the financial support of the University of California at Berkeley and the Dutch Technology Foundation. This support is gratefully acknowledged. The Richmond Field data was obtained with the help of John Washbourne, Qicheng Dong and Tao Zhen of the Engineering Geoscience Group at the Lawrence Berkeley National Laboratory. Their assistance was invaluable in this "Dutch day in the field" with a lot of rain and mud. The equipment used during the experiment was made available by Geometries Inc.

REFERENCES

Blonk, B., Herman, G.C., and Drijkoningen, G.G., 1995, An elastodynamic inverse scattering method for removing scattered surface waves from field data: Geophysics, 60, 1897-1905.

Blonk, B., and Herman, G.C., 1996, Removal of scattered surface waves using multicomponent seismic data: Geophysics, 61, 1483-1488.

Mars, J.I., and Rector, J.W., 1995, Constrained eigenvectors: A means to separate aliased arrivals: 65th Ann. Internat. Mtg., Soc. Expl. Geophys., Expanded Abstracts, 49-52.

Steeples, D.W., Green, A.G., McEvilly, T.V., Miller, R.D., Doll, W .E., and Rector, J.W., 1997, A workshop examination of shallow seismic reflection surveying: The Leading Edge, 16, 1641-1647.